Effects of Jasplakinolide on the Kinetics of Actin Polymerization

AN EXPLANATION FOR CERTAIN *IN VIVO* OBSERVATIONS*

Michael R. Bubb‡, Ilan Spector§, Bret B. Beyer, and Katina M. Fosen

From the Department of Medicine, University of Florida, Gainesville, Florida 32610 and the §Department of Physiology and Biophysics, State University of New York, Stony Brook, New York 11794

Jasplakinolide paradoxically stabilizes actin filaments *in vitro*, but *in vivo* it can disrupt actin filaments and induce polymerization of monomeric actin into amorphous masses. A detailed analysis of the effects of jasplakinolide on the kinetics of actin polymerization suggests a resolution to this paradox. Jasplakinolide markedly enhances the rate of actin filament nucleation. This increase corresponds to a change in the size of actin oligomer capable of nucleating filament growth from four to approximately three subunits, which is mechanistically consistent with the localization of the jasplakinolide-binding site at an interface of three actin subunits. Because jasplakinolide both decreases the amount of sequestered actin (by lowering the critical concentration of actin) and augments nucleation, the enhancement of polymerization by jasplakinolide is amplified in the presence of actin-monomer sequestering proteins such as thymosin β_4. Overall, the kinetic parameters *in vitro* define the mechanism by which jasplakinolide induces polymerization of monomeric actin *in vivo*. Expected consequences of jasplakinolide function are consistent with the experimental observations and include *de novo* nucleation resulting in disordered polymeric actin and in insufficient monomeric actin to allow for remodeling of stress fibers.

Jasplakinolide is a cyclic peptide isolated from the marine sponge, *Jaspis johnstoni*, that we have previously shown to bind to and stabilize filamentous actin *in vitro* (1). *In vivo* data suggests that jasplakinolide-treated prostate cancer cells have both decreased labeling of F-actin and decreased amounts of rhodamine-phalloidin bound to cell extracts (2), results that could be explained by the observation that jasplakinolide and phalloidin bind competitively to actin (1). In addition, however, *in vivo* data also convincingly show that jasplakinolide disrupts actin filaments with alterations in cellular architecture (2, 3), an effect that cannot be explained simply by competitive binding. We now present kinetic data characterizing the steady state and time-dependent *in vitro* interactions between jasplakinolide and actin that provide a plausible explanation for the effects of jasplakinolide on actin distribution in cultured cells.

EXPERIMENTAL PROCEDURES

Materials—Rabbit skeletal muscle actin was prepared from frozen muscle (Pel-Freez, Rogers, AR) in buffer G (5.0 mM Tris, 0.2 mM ATP, 0.2 mM dithiothreitol, 0.1 mM CaCl$_2$, and 0.01% sodium azide, pH 7.8) (4). Non-muscle actin from bovine brain was prepared by the method of Ruscha and Himes (5). Muscle and non-muscle pyrenyl-labeled actins[1] were prepared with 0.67–0.95 mol of label/mol of protein using the method of Kouyama and Mihashi (6). Labeled and unlabeled actins were further purified by gel filtration on Superose 12 (Amersham Pharmacia Biotech). Thymosin β_4 cDNA was a gift from Dr. Vivian Nachmias and was inserted in a pET-11a vector, expressed in BL21(DE3) *Escherichia coli*, and purified as described previously (7). Jasplakinolide was a gift from Drs. Phillip Crews and Yoel Kashman or was purchased from Molecular Probes (Eugene, OR) and was diluted in Me$_2$SO to 100 μM for the *in vivo* experiments and to 1.41 mM for the *in vitro* experiments.

Cell Culture and Fluorescence Microscopy—Rat embryonic fibroblasts (REF52) were grown on glass coverslips in 90% Dulbecco's modified Eagle's medium, 10% fetal bovine serum, and antibiotics (50 IU penicillin and 50 μg/ml streptomycin) at 37 °C in a humidified atmosphere of 5% CO$_2$. Jasplakinolide was added to the cells at final concentrations of 50–300 nM, and cells were examined over a 1–24-h period. For F-actin staining treated and untreated cells were washed 2× in PBS, fixed with 3.7% formaldehyde in PBS for 15 min at 21 °C, washed 3× with PBS, and permeabilized by dipping in acetone at −20 °C for 5 min. After permeabilization, Texas Red phalloidin solutions (Molecular Probes Inc.) were applied to the cells for 20 min at 21 °C. REF52 cells were then washed 4× with PBS and mounted on microscope slides in a Vectashield mounting medium with DAPI (Vector Laboratories Inc.) to visualize the nucleus. Cells were examined by epifluorescence with a Nikon Diaphot microscope with 63× oil immersion lens using a three-dye filter set (DAPI/fluorescein/Texas Red) (Omega Optical) and photographed using Kodak Gold MAX print film or Elite Chrome 400 slide film. Color prints and slides were digitally scanned and transferred to Adobe Photoshop 5.0 software for color channels splitting and figure assembly.

Stabilization of F-actin—Pyrenyl-labeled rabbit muscle actin or bovine brain actin was converted to Mg^{2+}-actin by the addition of 125 μM EGTA and 50 μM MgCl$_2$ and after 15 min was polymerized to Mg^{2+}-F-actin (20 μM) by the addition of MgCl$_2$ to 2.0 mM. The time course of depolymerization was followed after dilution of actin to 2.2 μM in Mg-G buffer (buffer G plus 50 μM MgCl$_2$ and 125 μM EGTA) at 22 °C in a steady state fluorimeter with excitation 365.6 and emission 386.6 nm. Samples were removed from the fluorimeter, and Me$_2$SO or concentrated stock solution of jasplakinolide in Me$_2$SO was added at 75 s, and the samples were mixed and returned to the fluorimeter at 90 s.

Steady State Kinetics and Determination of Actin Subunit On- and Off-rates—Actin (5% pyrenyl-actin) was converted to Mg^{2+}-actin as before and was polymerized by the addition of MgCl$_2$ to 0.35 mM (final actin concentration, 20 μM). Individual samples were made by dilution of the original stock of F-actin without a change in buffer conditions, and the final fluorescence (same conditions as for the stabilization assay) was read at 4 and 24 h after dilution. For the measurement of elongation rates, gel-filtered cross-linked F-actin seeds were prepared as described previously (8) by cross-linking (unlabeled) F-actin with *N,N'*-phenylenebismaleimide and pooling the gel-filtered fractions containing actin oligomers. Prior to the experiments employing jasplakinolide, preliminary data confirmed that the initial rate of polymerization was proportional to both the concentration of added seeds and to the concentration of free actin, which was large relative to the critical

[1] The abbreviations used are: pyrenyl-actin, actin labeled on Cys-374 with *N*-(1-pyrene)iodoacetamide; REF52, rat embryonic fibroblast 52; PBS, phosphate-buffered saline; DAPI, 4,6-diamidino-2-phenylindole.

concentration of actin (see Equation 2 below). Actin (5% pyrenyl-actin) was converted to Mg^{2+}-actin in a glass cuvette. After 15 min, jasplakinolide, seeds, and $MgCl_2$ to a final concentration of 0.35 mM were all added simultaneously; the samples were mixed and the fluorescence intensity was measured as a function of time. At fixed total actin concentration, the initial slope of the fluorescence change was assumed to be proportional to the elongation rate (8). Depolymerization rates were measured using Mg^{2+}-F-actin stock as for steady state measurements, with dilution to 3 μM with varying concentrations of jasplakinolide. Latrunculin (5.0 μM) was added to the diluted sample to keep the free G-actin concentration less than 0.05 μM during the time it took the first 10% of F-actin to depolymerize. The fluorescence change was linear over this time interval, consistent with the assumptions that few filaments completely depolymerized in this amount of time and that re-addition of subunits to polymer was negligible (9, 10).

Polymerization Time Course—Actin (5%-pyrenyl-actin) was converted to Mg^{2+}-actin, and polymerization was induced with the addition of $MgCl_2$ to a final concentration of 2.0 mM (or in some cases, 2.0 mM $MgCl_2$ with 100 mM KCl), and the time course was followed at 22 °C. The time course of polymerization was modeled as summarized by Tobacman and Korn (11) with implicit assumptions as detailed by Bubb and Korn (12), including the specific assumption that the concentration of oligomeric species of actin are negligible during the entire polymerization reaction. This assumption is specifically addressed in the current work in experiments employing sedimentation velocity. In brief, the rates of nucleation, $d[C_n]/dt$, and elongation, $d[A_f]/dt$, are defined by two differential equations (Equations 1 and 2).

$$d[C_n]/dt = K_n \cdot k_c^+ \cdot [A]^{(N-1)} \cdot ([A] - C_c) \qquad \text{(Eq. 1)}$$

$$d[A_f]/dt = k_c^+ \cdot [C_n] \cdot ([A] - C_c) \qquad \text{(Eq. 2)}$$

where $[C_n]$ is the molar concentration of nuclei; $[A_f]$ is the concentration of polymerized actin subunits; $[A]$ is the actin monomer concentration; k_c^+ is the sum of the rate constants for elongation at the two filament ends; C_c is the critical concentration of actin; and N is the number of subunits in a nucleus, *i.e.* the smallest aggregate for which elongation is more likely than dissociation. Numerical integration of Equations 1 and 2 produces a curve for the time course of polymerization that is dependent on the actin concentration, the critical concentration, and a parameter $K_n \cdot (k_c^+)^2$. The value for C_c was determined experimentally from steady state data as described later; therefore, for a given value of N, the only parameter required to fit data for the time course of polymerization is the product of $K_n \cdot (k_c^+)^2$. In the absence of jasplakinolide, the best fit to data for the time course of actin polymerization was previously shown to occur with $n = 4$ (11).

The time course in the presence of thymosin β_4 is modeled with the additional assumption that actin monomer binds to thymosin β_4 to form a complex that does not interact with F-actin. The interaction between thymosin β_4 and actin, with equilibrium dissociation constant K_d, is assumed to maintain a rapid equilibrium with respect to the polymerization reaction.

Sedimentation Velocity—Actin (15 μM) was incubated in Mg-G buffer at 4 °C for 24 h alone or with 15 μM phalloidin or 2 μM jasplakinolide. Samples of 400 μl were loaded into double sector analytical ultracentrifuge cells and were run in the Beckman XLA centrifuge at 53,000 rpm at 4 °C. Actin that cleared the meniscus within 7 min at 53,000 rpm, as determined from a comparison with a preliminary scan obtained at 3,000 rpm, was considered to be F-actin (13). Absorbance scans were obtained at 12- or 13-min intervals at 280 nm. Sedimentation coefficients were calculated using the second moment analysis method (14). Translational diffusion coefficients were determined according to the procedure of Muramatsu and Minton (15), utilizing the function $z(t) = \pi \cdot d \cdot t/4 + K$, where $z(t)$ is a nearly linear transformation of the theoretical gradient predicted by Fick's law of diffusion for a homogeneous solute. The translational diffusion coefficient, d, is then $4/\pi$ times dz/dt, and $d_{20,w}$ is calculated using interpolated values for viscosity and density of 5 mM Tris obtained from standard tables. At these actin concentrations, the hydrodynamic coefficients can be assumed to be independent of actin concentration (16).

RESULTS

Jasplakinolide Induces Distinctive Concentration- and Time-dependent Effects on Actin Distribution of REF52 Cells—The distribution of F-actin in untreated cells (Fig. 1A) shows a dense network of parallel stress fibers that remained intact following 2 h exposure to 50 (Fig. 1B) or 100 nM (Fig. 1C)

jasplakinolide. With 50 nM there was only a slight increase in the fluorescence intensity of F-actin bundles in the cell center, and the short term effects of 100 nM were manifest by the formation of actin aggregates at the perinuclear region. However, exposure of cells to 200 nM jasplakinolide for 2 h (Fig. 1D) resulted in almost complete depletion of F-actin from the central region of many cells, which assumed a diamond shape and displayed thick F-actin bundles and aggregates at the cell margins. Exposure of cells to 50 and 200 nM jasplakinolide for 24 h resulted in the appearance of large masses of F-actin. However, although with 50 nM cell shape was not altered, stress fibers were still visible, and the actin masses were clumped primarily in the perinuclear region (Fig. 1E), and with 200 nM, cells contracted and most stress fibers disappeared and were replaced by large F-actin masses that were located either in the perinuclear region or in the two poles of the cell (Fig. 1G).

Jasplakinolide Rapidly Binds to and Stabilizes F-actin—Jasplakinolide prevented depolymerization of both rabbit skeletal muscle and bovine brain actin in a dose-dependent manner (Fig. 2). The time required to achieve stabilization of F-actin was less than or equal to the time required to mix the samples (15 s). Previously we had reported that jasplakinolide binds to muscle F-actin with K_d of 15–300 nM (1). The continuation of the dose response to 2.0 μM for both muscle and non-muscle actin without saturation suggests that F-actin has at least a few binding sites with much lower affinity than previously reported that must be saturated to provide maximal inhibition of depolymerization. Perhaps at nearly full occupancy of binding sites along a filament, additional binding of jasplakinolide occurs only with negative cooperativity.

Steady State Fluorescence Intensity Data Show That Jasplakinolide Decreases the Critical Concentration of Actin—Four hours after the addition of jasplakinolide to Mg^{2+}-F-actin, jasplakinolide causes a dose-dependent decrease in the critical concentration of actin from 1.8 μM to 0.8 and 0.2 μM by 0.15 and 0.30 μM jasplakinolide, respectively (Fig. 3A). After 24 h the data show that even at low jasplakinolide concentrations, C_c is decreased to 0.2 to 0.4 μM (Fig. 3B). At 24 h the effect of jasplakinolide no longer shows a dose response, suggesting saturation of relevant binding sites even at the lowest concentration (0.15 μM). The $MgCl_2$ concentration of 0.35 mM was chosen specifically to provide a high enough value of C_c in the absence of drug, so that any decreases caused by jasplakinolide could be accurately measured.

The Decrease in Critical Concentration Is Mediated Largely by a Decrease in the Dissociation Rate of Actin Subunits, with a Small Increase in the Rate of Elongation—Jasplakinolide increased the rate constant for elongation in a seeded polymerization assay by a factor of up to 2 (Fig. 4). This effect was saturable at low concentrations of jasplakinolide ($\sim$100 nM). Jasplakinolide caused less than a 5% increase in the elongation rate in the absence of seeds, *i.e.* for the conditions employed in the elongation assay, jasplakinolide did not nucleate filament growth (data not shown). As another control, elongation rates measured with the same concentrations of phalloidin replacing jasplakinolide caused a 0–20% increase in the elongation rate (data not shown), consistent with a previous report (17). The effects of jasplakinolide on the depolymerization rate constant (from both filament ends), k_c^-, showed a nearly linear dependence on jasplakinolide concentration up to the highest concentration employed (0.3 μM), but since the total actin concentration was 3.0 μM, these values do not represent saturation of filament-binding sites (Fig. 4). The relative rate constants k_c^+ and k_c^- provide values for calculation of C_c, demonstrating a 6.2-fold decrease in C_c at 0.15 μM jasplakinolide and 20-fold decrease at 0.3 μM jasplakinolide (Fig. 4, *inset*). The disparity
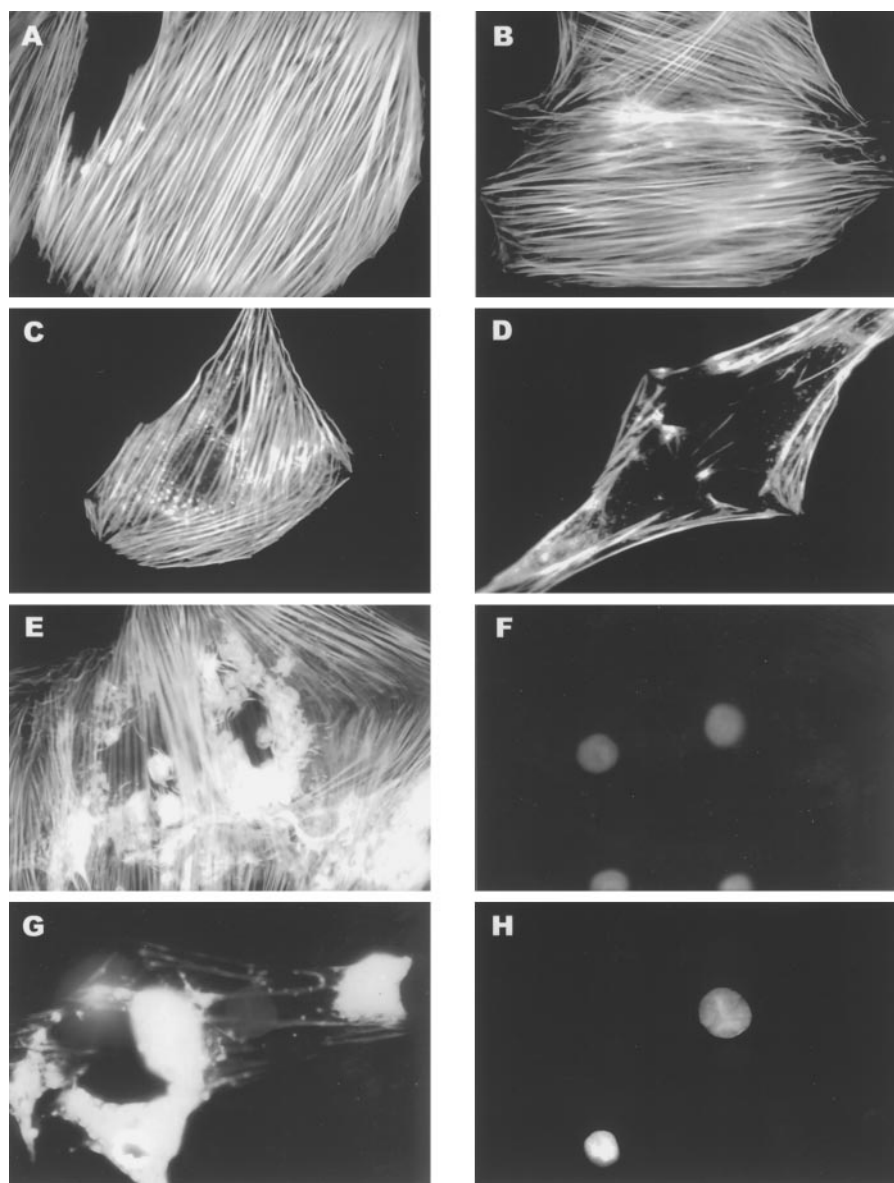
FIG. 1. **Concentration- and time-dependent effects of jasplakinolide on REF52 cells.** Fluorescence images of REF52 cells labeled with Texas Red phalloidin to visualize actin filaments (*A–E* and *G*) and with DAPI to visualize the nucleus (*F* and *H*) are shown. *A*, control cells; *B–D*, cells treated for 2 h with 50 nM jasplakinolide (*B*); 100 nM jasplakinolide (*C*), and 200 nM jasplakinolide (*D*). *E–H*, cells treated for 24 h with 50 nM jasplakinolide (*E* and *F*) and 200 nM jasplakinolide *G* and *H*.

between these results and those for steady state measurements is discussed later.

The Effects of Jasplakinolide on the Time Course of Actin Polymerization Demonstrate a Decrease in the Size of an Effective Nucleus to Three Subunits—As previously demonstrated, jasplakinolide augments the rate of polymerization of Mg^{2+}-actin (Fig. 5*A*). For comparison, in the absence of jasplakinolide, 1.3 μM actin exhibited a 5-fold increase in fluorescence after 2000 s (data not shown), but a similar 5-fold increase occurred after 80 s in the presence of 2.0 μM jasplakinolide (Fig. 5*A*). Varying concentrations of Mg^{2+}-actin polymerized with 2.0 μM jasplakinolide can be modeled reasonably well assuming a nucleus (*N*) of 3 subunits (Fig. 5*A*) and a critical concentration of zero (calculated at steady state as in Fig. 3; data not shown). Then, $K_n \cdot (k_c^+)^2 = 9.4 \cdot 10^{13}$ s^{-2} M^{-3}. When assuming a nucleus of 4 subunits, the data can be best fit with $K_n \cdot (k_c^+)^2 = 1.8 \cdot 10^{20}$ s^{-2} M^{-4}, but the model then predicts that polymerization will occur faster than observed for total actin concentrations of more than 0.8 μM and slower than observed for less than 0.5 μM (Fig. 5*A*). Not shown in Fig. 5*A* is the observation that individual curves vary slightly on repetition (Fig. 5*B* does give an indication of the variability between samples), but in three series of assays, the observation that the data could be

better fit with *N* of 3 than *N* of 4 was true for each series.

The differential equations for nucleation-elongation kinetics predicts that the size of the nucleus can be determined from an ln/ln plot of the actin concentration *versus* the time to reach a fixed percentage of polymerized actin (11, 18). Then, assuming the free actin concentration is large relative to the critical concentration, the slope is one-half the nucleus size. This assumption is satisfied employing data (done in triplicate) as shown in Fig. 5*A*. The time required for 50% of the actin to polymerize was utilized, and the results are plotted in Fig. 5*B*. Control data in the absence of jasplakinolide show a slope of 1.98, consistent with previous reports of a tetrameric nucleus (11), whereas the data for 2.0 μM jasplakinolide show a slope of 1.62, most consistent with a trimeric nucleus. A comparison of phalloidin (2.0 μM) with jasplakinolide in the same series of assays showed, as previously reported for Ca^{2+}-actin (17), that phalloidin had only a minor effect on the rate of unseeded filament assembly of Mg^{2+}-actin but did cause a modest reduction in slope to 1.79 (Fig. 5*B*).

The binding site for phalloidin on actin has been previously identified and is at the interface of three actin subunits (19). The finding that jasplakinolide stabilizes an actin trimer sufficiently to ensure that it will elongate rather than dissociate
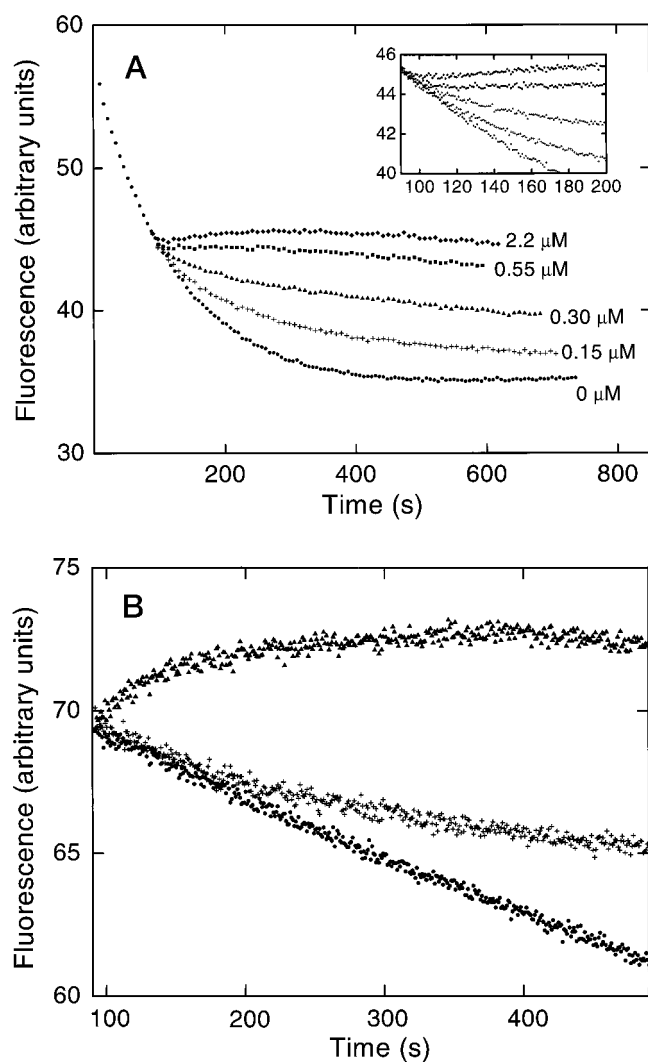
FIG. 2. **Time course of actin stabilization by jasplakinolide as monitored by fluorescence.** *A*, pyrenyl-labeled rabbit muscle Mg^{2+}-F-actin diluted to 2.2 μM. After 75 s, jasplakinolide was added. The samples were mixed and replaced in the fluorimeter after 90 s to give final jasplakinolide concentrations of 2.2 μM ($\blacklozenge$), 0.55 μM ($\blacksquare$), 0.30 μM ($\blacktriangle$), 0.15 μM (+), or 0 μM ($\bullet$) jasplakinolide. *Inset*, an expanded view of the same data including the time immediately after the addition of jasplakinolide. *B*, pyrenyl-labeled bovine brain Mg^{2+}-F-actin diluted to 2.2 μM as in *A* for 2.0 μM ($\blacktriangle$), 0.50 μM (+), and 0.15 μM ($\bullet$) jasplakinolide. The data for 0.15 μM jasplakinolide were indistinguishable from those in the absence of jasplakinolide.

might have been anticipated if jasplakinolide binds at the same site as phalloidin. Whereas it has been proven that jasplakinolide binds competitively with phalloidin (1), there is no direct evidence that the two drugs compete for the same binding site.

Effects of Jasplakinolide Are Amplified in the Presence of Thymosin β_4—At a fixed concentration of Mg^{2+}-actin (1.3 μM) and jasplakinolide (2.0 μM), varying concentrations of thymosin β_4 were added prior to initiation of polymerization with a final concentration of 2.0 mM $MgCl_2$ (Fig. 6A). For comparison, the polymerization of 1.3 μM Mg^{2+}-actin was nearly completely inhibited by 3.0 μM thymosin β_4 in the absence of jasplakinolide, with an increase in fluorescence intensity of approximately 2% in 1500 s (Fig. 6A). Steady state fluorescence intensity was measured in the presence of thymosin β_4 after 24 h (Fig. 6A, *inset*).

The effects of jasplakinolide on the steady state F-actin concentration in the presence of thymosin β_4 do not fit perfectly with a model of sequestration of actin by thymosin β_4 in a 1 to
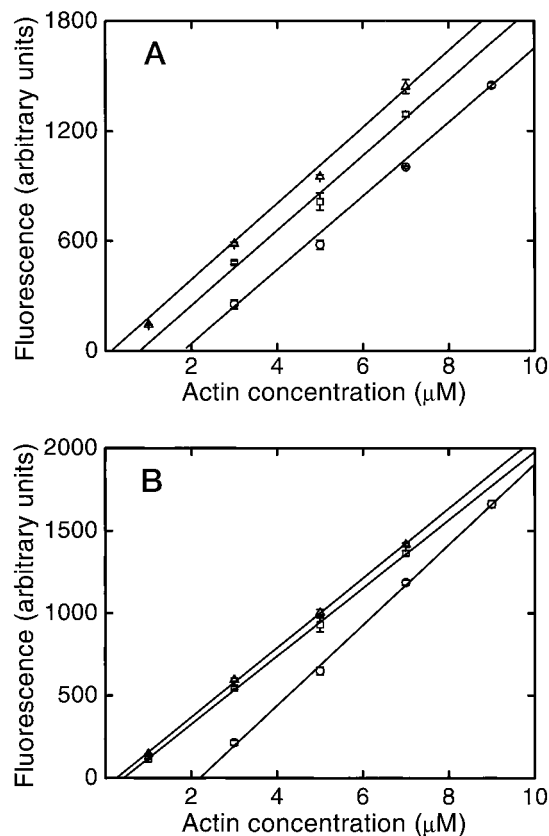

FIG. 3. **Critical concentration determination of actin polymerization at steady state equilibrium as monitored by fluorescence.** Data shown for 0.3 μM ($\triangle$), 0.15 μM ($\square$), and 0 μM ($\bigcirc$) jasplakinolide with 2.2 μM Mg^{2+}-actin (5% pyrene-labeled) in 0.35 mM $MgCl_2$. *A*, fluorescence intensity after 4 h. On the basis of the *x* intercepts, the C_c for actin polymerization was lowered from 1.8 to 0.8 μM with the addition of 0.15 μM jasplakinolide and to 0.2 μM with the addition of 0.3 μM jasplakinolide. *B*, steady state fluorescence intensity after 24 h. *Error bars* represent $\pm\sigma$ for three independent experiments.
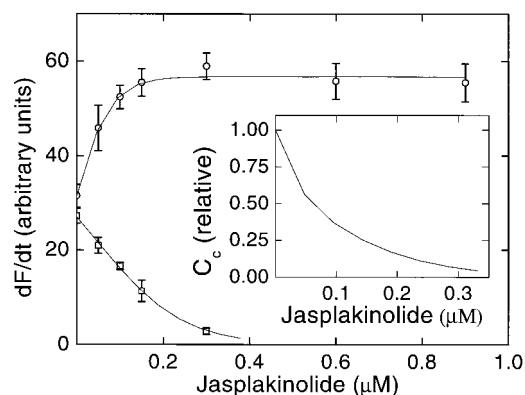

FIG. 4. **Relative elongation and depolymerization rates with jasplakinolide.** Elongation rates are increased modestly by jasplakinolide, with saturation at low concentrations of drug (*circles*). Depolymerization rates (*squares*) are shown as a function of jasplakinolide concentration. The curves through the data are arbitrary. *Error bars* represent $\pm 2\sigma$ for three independent experiments. *Inset*, critical concentration as a function of jasplakinolide concentration (relative to C_c for no jasplakinolide).

1 stoichiometric complex (compare *solid* and *dashed line,* Fig. 6A, *inset*). The best fit to such a model suggests a K_d of 0.39 μM for thymosin β_4 and actin monomer. Additionally, modeling the entire time course of polymerization of actin assuming values for K_n, k_c^+, and C_c as determined in Fig. 5A and assuming rapid equilibrium binding of thymosin β_4 to actin with $K_d = 0.39$ μM
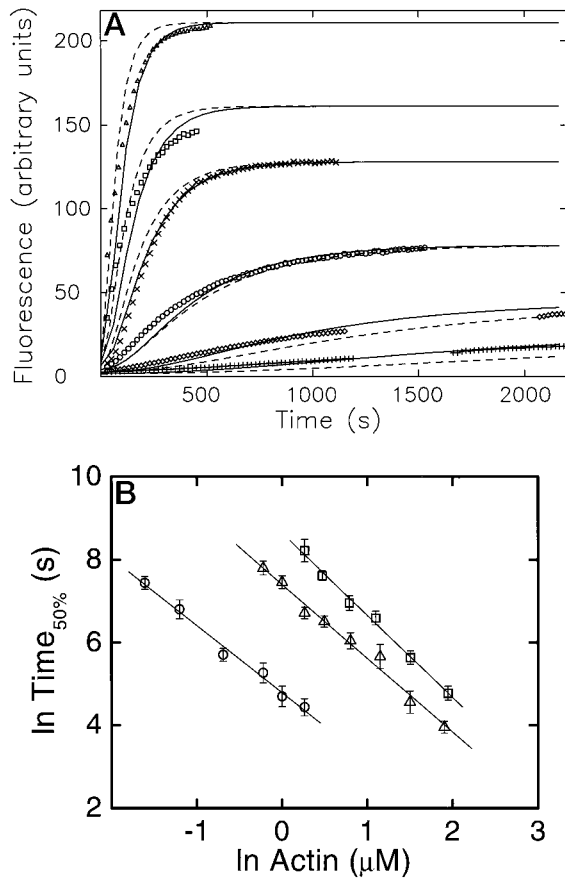
FIG. 5. **Time course of Mg²⁺-actin polymerization in the presence of jasplakinolide.** *A*, polymerization of 5% pyrenyl-Mg²⁺-actin at various actin concentrations (1.3 μM, *triangles*; 1.0 μM, *squares*; 0.8 μM, *x-shaped symbols*; 0.5 μM, *circles*; 0.3 μM, *diamonds*; 0.2 μM +*-shaped symbols*) with 2.0 μM jasplakinolide. The best global fit to the data using a nucleus of three subunits, $N = 3$ (*solid lines*), is superior to the comparable best fit with $N = 4$ (*dashed lines*). *B*, the time to reach 50% of the final change in fluorescence ($t_{50\%}$) was determined for data as in *A* done in triplicate, and also for control polymerization curves obtained in the absence of jasplakinolide. For comparison, results for polymerization in the presence of 2.0 μM phalloidin show a much less potent effect on nucleation. The *solid lines* show the least squares fit to the data and have slope of 1.62 for 2.0 μM jasplakinolide (○), 1.79 for 2.0 μM phalloidin (△), and 1.98 in the absence of drug (□). The *error bars* represent ±2σ for three independent determinations.

FIG. 6. **Time course of Mg²⁺-actin polymerization in the presence of jasplakinolide and thymosin β_4.** *A*, polymerization curves are shown for 1.3 μM 5% pyrenyl-Mg²⁺-actin and 2.0 μM jasplakinolide in 2.0 mM MgCl₂. Thymosin β_4 concentration is variable at 0 μM (▽), 1 μM (□), 3 μM (+), 5 μM (○), and 12 μM (△). A control polymerization curve shows the results for 3 μM thymosin β_4 in the absence of jasplakinolide (◇). *Inset*, fluorescence intensity at steady state for various concentrations of thymosin β_4. (Not all concentrations are depicted in the larger figure.) The *solid line* shows the best fit to a model in which thymosin β_4 sequesters actin in a 1 to 1 complex with K_d of 0.39 μM. The *dashed line* arbitrarily connects the data points in order to highlight the systematic deviation from the theoretical model. The *error bars* represent ±σ for three independent experiments. *B*, in a physiologic buffer containing 100 mM KCl, polymerization of 3.0 μM pyrenyl-Mg²⁺-actin to steady state in the presence of 6.0 μM thymosin β_4 (□) results in a similar fluorescence intensity to that obtained with 1.1 μM Mg²⁺-actin alone (○), with the steady state fluorescence levels shown prior to $t = 0$. Addition of 3.0 μM jasplakinolide at $t = 0$ results in a large increase in fluorescence intensity only for the sample containing thymosin β_4. *Inset*, actin at 1 μM (□) initially polymerizes at the same rate as 2.8 μM thymosin β_4 and 3.0 μM actin (○) in physiologic buffer (*closed symbols*). At the same protein concentrations, 2.0 μM jasplakinolide induces more rapid and extensive polymerization in the sample containing thymosin β_4 (*open symbols*).

produces results different from those observed. For example, a solution to the differential Equations 1 and 2 predicts that in the presence of 3 μM thymosin β_4, 2.0 μM jasplakinolide, and 1.3 μM actin, approximately 5% of the actin would polymerize after 1000 s, in contrast to the observed rate (18% polymerized at 1000 s) demonstrated in Fig. 6A. Therefore the combination of a lower critical concentration with less sequestered actin and the large increase in $K_n \cdot (k_c^+)^2$ are not entirely sufficient to explain the ability of jasplakinolide to induce polymerization in the presence of thymosin β_4. Apparently, actin bound to thymosin β_4 is participating in the polymerization process, either during nucleation or elongation. Previous investigators have suggested that this might also be the case in the absence of jasplakinolide (7), but others have not found evidence for anything other than monomer sequestration by thymosin β_4 (20). A previous report (21) that thymosin β_4-actin complexes could directly associate with phalloidin-stabilized actin neglected the fact that phalloidin, like jasplakinolide, lowers the critical concentration and therefore decreases the amount of actin sequestered by thymosin β_4 (17).

Since jasplakinolide both decreases the critical concentration of actin (Figs. 3 and 4) and accelerates nucleation (Fig. 5), the
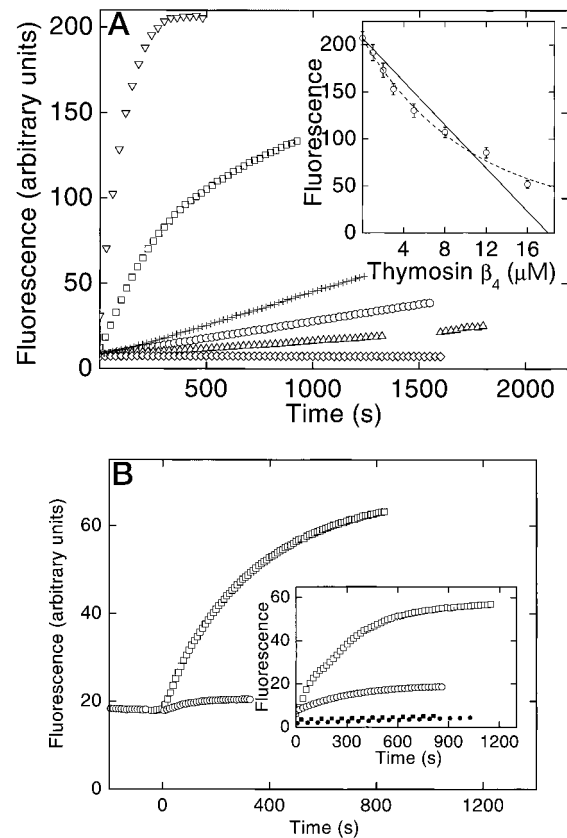
effects of jasplakinolide on actin polymerization should be amplified in the presence of thymosin β_4, where the drop in critical concentration should free up actin that would have been sequestered by thymosin β_4 in the absence of jasplakinolide. Indeed, a comparison of Figs. 5A and 6A shows that at a total actin concentration of 1.3 μM, the maximum slope for actin polymerization is increased approximately 40-fold by 2.0 μM jasplakinolide (Fig. 2), whereas the comparative slopes in the presence of 3 μM thymosin β_4 show a 300-fold difference (Fig. 6A).

The effect of the addition of jasplakinolide under physiological conditions to cells rich in thymosin β_4 can be illustrated *in vitro* (Fig. 6B). Adding jasplakinolide to polymerized Mg²⁺-actin in a physiologic buffer (2.0 mM MgCl₂ and 100 mM KCl) at steady state results in only a slight increase in polymer corresponding to a drop in critical concentration. However, adding
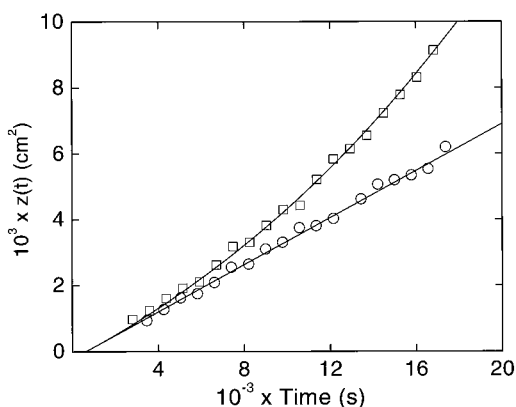
FIG. 7. **Diffusion coefficients for non-polymeric actin with jasplakinolide or phalloidin.** Mg^{2+}-actin (15 μM) incubated with either 2 μM jasplakinolide (*circles*) or 15 μM phalloidin (*squares*) and subjected to sedimentation velocity is shown. The initial scan at 12 min showed the rapid sedimentation of polymeric actin, which accounted for about 20% of the actin for each sample. Sedimentation coefficients for the remaining non-polymeric actin were similar for the two samples ($s_{20,w}^0$ = 3.2 in jasplakinolide; 3.5 in phalloidin). The linear transformation, $z(t)$, was applied to successive scans, with dz/dt proportional to the translational diffusion coefficient. The changing slope of the arbitrary curve drawn through the data for phalloidin-treated actin most likely represents sample heterogeneity.

jasplakinolide to a sample in the same buffer with the same amount of Mg^{2+}-F-actin (and therefore, approximately the same initial fluorescence intensity), but with additional actin sequestered by thymosin β_4, results in a rapid and large increase in actin polymer. The amplification of the effect of jasplakinolide in the presence of thymosin β_4 can be best explained by the hypothesis that jasplakinolide markedly decreases the critical concentration of actin, resulting in an abrupt decrease in the amount of actin sequestered by thymosin β_4. In fact, the steady state level of fluorescence achieved after the addition of 3.0 μM jasplakinolide to a sample with 3.0 μM actin is independent of the concentration of thymosin β_4, implying that to the extent measurable, there is no actin sequestered by thymosin β_4 in a physiologic buffer after addition of jasplakinolide, *i.e.* the critical concentration is effectively zero (data not shown). If the actin concentration is adjusted so that the initial rate of polymerization of Mg^{2+}-actin in physiologic buffer (2.0 mM $MgCl_2$ and 100 mM KCl) is similar in the presence (3.0 μM actin) and absence (1.0 μM actin) of 2.8 μM thymosin β_4, then the same samples polymerized in the presence of 2.0 μM jasplakinolide are markedly different (Fig. 6B, *inset*). A much greater extent of polymerization is observed in the sample containing thymosin β_4 as a consequence of the drop in critical concentration.

Jasplakinolide and Phalloidin Markedly Diminish the Concentration of Actin Oligomers at Actin Concentrations Near That of the Critical Concentration—Conditions were determined in which approximately 20% of 15 μM actin would pellet as F-actin during sedimentation velocity experiments, implying a critical concentration of about 12 μM. In Mg-G buffer with a 24 h incubation, this required either 2 μM jasplakinolide or 15 μM phalloidin. Residual non-polymeric actin sedimented as though largely monomeric for both the jasplakinolide- and phalloidin-treated actin. The sedimentation coefficients of the monomeric fraction in the presence of jasplakinolide was similar to that previously reported for monomeric actin ($s_{20,w}^0$ = 3.2) (8). The diffusion coefficient for the non-polymeric fraction of actin treated with jasplakinolide was also consistent with expectations for an actin monomer ($D_{20,w}^0$ = 7.53; Fig. 7) (22). The phalloidin-treated actin yielded a slightly larger sedimentation coefficient ($s_{20,w}^0$ = 3.5) and an indeterminate diffusion

coefficient related to dispersion of a heterogeneous sample, both results being consistent with the presence of a small percentage of oligomeric actin. In the presence of either drug, the oligomer content was much lower than that previously reported by Atrii *et al.* (13) for Mg^{2+}-actin at a similar critical concentration, for which actin oligomers accounted for 91% of the non-polymeric fraction.

DISCUSSION

Previous work has shown that jasplakinolide decreases F-actin labeling *in vivo* with alterations in cellular morphology and decreases rhodamine-phalloidin binding in extracts of prostate cancer cells (2), that it induces actin polymerization in blue algae (23), and that it causes the formation of F-actin aggregates in *Dictyostelium discoideum* (24). As we observed, high concentrations of jasplakinolide have been reported to increase the density of actin filaments adjacent the plasma membrane in both smooth muscle and Madin-Darby canine kidney cells (25, 26), and this is accompanied by the loss of stress fibers in smooth muscle cells (26). Our description of changes in cellular architecture of fibroblasts after jasplakinolide treatment is consistent with those seen in epithelial cells (3). The effects of jasplakinolide on nucleation are consistent with the observed accumulation of disorganized aggregates of F-actin observed *in vivo*, both in concentration and time dependence. The spontaneous induction of nucleation sites by jasplakinolide would be expected to circumvent regulated actin filament elongation at filament ends. The effects of jasplakinolide on stress fibers can be explained by its ability to deplete G-actin, first by inducing the release of actin sequestered by thymosin β_4 (or other actin-sequestering proteins) and then by nucleation of filament assembly, leading to a cellular environment in which there is insufficient polymerization-competent G-actin to maintain stress fibers during normal turnover (27, 28). The prior observation that jasplakinolide decreases the cellular pool of identifiable G-actin (25, 26, 29) correlates with the expected drop in both free and sequestered G-actin caused by jasplakinolide *in vitro*. Phalloidin, without a large effect on the rate constant for nucleation (17), has been reported to induce similar changes in stress fibers when loaded directly into cells at high concentrations (30).

Our work suggests that the variations in the timing and extent of jasplakinolide-induced aggregate formation among differing cell types may be dependent on the pre-existing concentration of polymerization-competent G-actin. Cells that contain abundant stress fibers and relatively lower concentrations of G-actin show significant aggregate formation only after the remodeling of stress fibers sufficiently augments the G-actin pool to allow for jasplakinolide-induced filament nucleation. The assessment of polymerization-competent G-actin concentrations remains problematic as actin may be monomeric yet may not be polymerization-competent due to its spatial distribution (31), post-translational modifications (32), nucleotide content (33), or sequestration by actin-binding proteins that may not readily participate in polymerization, *e.g.* the high affinity profilactin complex (34).

Alternative, but more complex, explanations for the *in vivo* effects of jasplakinolide could be based on secondary effects of the drug. Alterations in G-actin have been shown to regulate the synthesis of actin and of other actin regulatory proteins (35). Jasplakinolide (at higher concentrations than employed here) has specifically been shown to activate serum response factor (29). A finite number of effects on actin-regulatory proteins could be postulated that would mimic those predicted by jasplakinolide-actin biochemistry and thus would be expected to produce the same *in vivo* observations. A series of experiments designed to detect the significance of protein synthesis to

jasplakinolide function and a measurement of the concentrations and activity of various actin-binding proteins to detect a correlation with morphological observations could theoretically determine the significance of these secondary effects on jasplakinolide function *in vivo*.

Several aspects of the kinetic analysis merit attention. As measured by its indirect effects on actin-filament stability, jasplakinolide binding to actin does not appear to be as slow as that reported for phalloidin (36), although direct measurements of association rate constants are not currently feasible. The steady state data signify a slow redistribution of jasplakinolide to sites that are most effective at decreasing C_c. Kinetically, this implies that an actin filament may present a large number of potential binding sites, all with similar association rate constants for jasplakinolide binding, but that certain sites have higher affinity at steady state and that jasplakinolide redistributes to these sites over time. These sites with relatively higher affinity are biologically relevant, as the steady state data suggest increased activity of jasplakinolide over time. Additionally, the high affinity sites can be saturated with low concentrations of jasplakinolide after 24 h but not at 4 h. A hypothesis explaining both the redistribution of jasplakinolide and the low concentration of jasplakinolide required for saturation would be that a small number of sites, perhaps at a filament end (or ends), have high affinity for jasplakinolide, and occupancy of these sites is responsible for decreasing C_c. The redistribution may be important in cell biological applications for jasplakinolide, as a large pool of F-actin *in vivo* may sequester jasplakinolide at binding sites that are not necessarily biologically active, *i.e.* jasplakinolide may bind indiscriminately along the length of actin filaments to sites with similar on-rates but lower overall affinity, after initially entering cells.

The difference in slopes between the lines drawn for the 24 h data with and without jasplakinolide is puzzling. An increase in F-actin concentration could be expected to result in dilution of jasplakinolide relative to filament subunit concentration and therefore a dilution of biological activity as suggested by the data. However, the binding sites responsible for lowering C_c appear to be saturated at all concentrations of actin, so dilution of jasplakinolide relative to active binding sites is not a reasonable explanation. Perhaps the decreasing apparent activity of jasplakinolide at higher total actin concentrations can be explained by lower affinity of jasplakinolide for pyrenyl-F-actin than for unlabeled F-actin. As for differences in binding of profilin to pyrenyl-G-actin and unlabeled G-actin, the artifact introduced by this difference would be expected to be diminished at the lowest concentrations of F-actin, where vanishingly small amounts of pyrenyl-actin would be excluded from the filament. However, similar differences in slope were observed when the experiment was repeated with 67% pyrenyl-actin (data not shown), making this explanation less likely. Still another possibility is that pyrenyl-F-actin has higher fluorescence when jasplakinolide occupies certain high affinity binding sites, with a greater artifact at low F-actin concentrations where the ratio of jasplakinolide to F-actin is highest. This would imply that the apparent decrease in critical concentration might be an artifact. This interpretation is ruled out by the finding that the addition of high concentrations of jasplakinolide to F-actin at steady state does not cause an immediate change in fluorescence intensity, and such a change would be expected to be immediate ($<$15 s) because of the relatively rapid association rate constant observed in Fig. 2.

Comparison of the steady state value of C_c (2.3–4.5-fold decrease at 0.15 μM jasplakinolide; 8–9-fold decrease at 0.3 μM) with the calculation of C_c from measurements k_c^+, and k_c^-

(6.2-fold decrease at 0.15 μM; 20-fold decrease at 0.3 μM) can be expected to result in certain inconsistencies. A trivial explanation might be that the 24-h steady state data for jasplakinolide are indeterminate because C_c is close to 0. (This would also imply that the apparent saturation by low concentrations of jasplakinolide is an artifact of the assay.) We think this is unlikely because our laboratory routinely measures lower values of critical concentrations in the range of 0.07 to 0.13 μM with a high degree of reproducibility (data not shown). Other explanations are available. The measurement of k_c^- is performed at actin concentrations less than C_c, yet there is evidence that k_c^- has a different value when the actin concentration is above or below the critical concentration, presumably related to differences in terminal subunit nucleotide content (37). The redistribution of jasplakinolide identified in the steady state data suggests another variable, so that the depolymerization experiment is analogous to the early (steady state 4 h data) distribution where jasplakinolide will bind nonselectively to all sites with similar on-rates but not necessarily those that result in either decreased C_c or k_c^-. In contrast, consistent with the evidence for saturation at low levels of jasplakinolide, the elongation data may represent selective binding to the relevant effector sites in this assay which is performed at a relatively high molar ratio of filament ends to filament subunits.

The apparent nucleation rate constants in the presence and absence of jasplakinolide cannot be directly compared because of the discrepancy in units due to the different values of N. However, for a given value of actin concentration in the mid-range of data in Fig. 2 for which the data can be adequately fit with N equal 4, the effective nucleation rate constants can be compared to give an estimate of the augmentation of nucleation by jasplakinolide. Thus for actin concentrations of 0.5 to 0.8 μM, the product of $K_n \cdot (k_c^+)^2$ when $N = 4$ ($1.8 \cdot 10^{20}$ s^{-2} M^{-4}) can be compared with the reported values for $K_n \cdot (k_c^+)^2$ in the absence of jasplakinolide ($1.7 \cdot 10^{16}$ s^{-2} M^{-4} determined using the same actin preparation (data not shown) and $6.0 \cdot 10^{15}$ s^{-2} M^{-4} as previously reported (12)) in the identical polymerization buffer. If the elongation rate, k_c^+, is augmented by a factor of about ~2 in the presence of jasplakinolide, then the relative increase in the apparent nucleation rate constant, $K_n \cdot k_c^+$, due to jasplakinolide is $1.8 \cdot 10^{20}/(1.7 \cdot 10^{16} \cdot 2)$ or $5 \cdot 10^3$.

Intuitively, one might expect that a drug that stabilizes actin oligomers in a helical conformation might result in an increase, rather than the observed decrease, in the concentration of actin oligomers found at total actin concentrations near the critical concentration. These results, however, can be qualitatively explained by the Oosawa-Kasai theory of helical polymerization (38). The concentration of linear oligomers found at any concentration of actin monomer will depend on K_l, the association constant for linear polymer. The association constant for helical polymer, K_h or $1/C_c$, is approximately constant for the conditions employed in the current work (*i.e.* $C_c \cong 12$ μM for both the jasplakinolide and phalloidin samples). If jasplakinolide and phalloidin increase K_h without significantly increasing K_l, as might be expected if these drugs bind at the interface of three subunits, then K_l in the presence of these drugs should be small relative to K_l for the conditions described by Attri *et al.* (13), as increasing Mg^{2+} would not be expected to selectively increase K_h. Since linear oligomers are predicted to account for the majority of oligomeric actin below the critical concentration, the small K_l can account for the decreased oligomer concentration in the presence of either jasplakinolide or phalloidin. The current results are not necessarily in conflict with those reported by Estes *et al.* (17) for phalloidin; the small amount of oligomer we observe may be helical and may serve as

effective nuclei for filament elongation, but the total amount of oligomer is much less than would be present if the critical concentration had been adjusted with divalent cation (as previously shown by others (13)) rather than phalloidin.

REFERENCES

1. Bubb, M. R., Senderowicz, A. M. J., Duncan, K. L. K, and Korn, E. D. (1994) *J. Biol. Chem.* **269,** 14869–14871
2. Sendarowicz, A. M. J., Kaur, G., Sainz, E., Laing, C., Inman, W. D., Rodriquez, J., Crews, P., Malspeis, L., Grever, M. R., Sausville, E. A., and Duncan, K. L. K. (1995) *J. Natl. Cancer Inst.* **87,** 46–51
3. Spector, I., Braet, F., Shochet, N. R., and Bubb, M. R. (1999) *Microsc. Res. Tech.* **47,** 18–37
4. Spudich, J. A., and Watt, S. (1971) *J. Biol. Chem.* **246,** 4865–4871
5. Ruscha, M. F., and Himes, R. H. (1981) *Prep. Biochem.* **3,** 351–360
6. Kouyama, T., and Mihashi, K. (1981) *Eur. J. Biochem.* **114,** 33–38
7. Carlier, M.-F., Didry, D., Erk, I., Lepault, J., Van Troys, M. L., Vandekerckhove, J., Perelroizen, I., Yin, H., Doi, Y., and Pantaloni, D. (1996) *J. Biol. Chem.* **271,** 9231–9239
8. Terry, D. R., Spector, I., Higa, T., and Bubb, M. R. (1997) *J. Biol. Chem.* **272,** 7841–7845
9. Kristofferson, D., Karr, T. L., and Purich, D. L. (1980) *J. Biol. Chem.* **255,** 8567–8572
10. Walsh, T. P., Weber, A., Davis, K., Bonder, E., Mooseker, M. (1984) *Biochemistry* **23,** 6099–6102
11. Tobacman, L. S., Brenner, S. L., and Korn, E. D. (1983) *J. Biol. Chem.* **258,** 8806–8812
12. Bubb, M. R., and Korn, E. D. (1995) *Biochemistry* **34,** 3921–3926
13. Attri, A. K., Lewis, M. S., and Korn, E. D. (1991) *J. Biol. Chem.* **266,** 6815–6824
14. Schachman, H. K. (1959) *Ultracentrifugation in Biochemistry*, pp. 75–81, Academic Press, New York
15. Muramatsu, N., and Minton, A. P. (1988) *Anal. Biochem.* **168,** 345–351
16. Lewis, M. S., Maruyama, K., Carroll, W. R., Kominz, D. R., and Laki, K. (1963) *Biochemistry* **2,** 34–39
17. Estes, J. E., Selden, L. A., and Gershman, L. C. (1981) *Biochemistry* **20,** 708–712
18. Oosawa, F., and Asakura, S. (1975) *Thermodynamics of the Polymerization of Protein,* pp. 47–51, Academic Press, New York
19. Heidecker, M., Yan-Marriott, Y., and Marriott, G. (1995) *Biochemistry* **34,** 11017–11025
20. Weber, A., Nachmias, V. T., Pennise, C. R., Pring, M., and Safer, D. (1992) *Biochemistry* **31,** 6179–6185
21. Reichert, A., Heintz, D., Voelter, W., Mihelic, M., and Faulstich, H. (1994) *FEBS Lett.* **347,** 247–250
22. Montague, C., Rhee, K. W., and Carlson, F. D. (1983) *J. Muscle Res. Cell Motil.* **4,** 95–101
23. Holzinger, A., and Meindl, U. (1997) *Cell Motil. Cytoskeleton* **38,** 365–372
24. Lee, E., Shelden, E. A., and Knecht, D A. (1998) *Cell Motil. Cytoskeleton* **39,** 122–133
25. Shurety, W., Stewart, N. L., and Stow, J. L. (1998) *Mol. Biol. Cell* **9,** 957–975
26. Patterson, R. L., van Rossum D. B., and Gill, D. L. (1999) *Cell* **98,** 487–499
27. Krendel, M. F., and Bonder, E. M. (1999) *Cell Motil. Cytoskeleton* **43,** 296–309
28. McGrath, J. L., Tardy, Y., Dewey, C. F., Jr., Meister, J. J., and Hartwig, J. H. (1998) *Biophys. J.* **75,** 2070–2078
29. Sotiropoulos, A., Gineitis, D., Copeland, J., and Treisman, R. (1999) *Cell* **98,** 159–169
30. Wehland, J., Osborn, M., and Weber, K. (1977) *Proc. Natl. Acad. Sci. U. S. A.* **74,** 5613–5617
31. Cao, L., Fishkind, D. J., and Wang, Y. (1993) *J. Cell Biol.* **123,** 173–181
32. Tsuyama, S., Inoue, Y., and Tanaka, M. (1997) *Int. J. Biochem. Cell Biol.* **29,** 293–310
33. Goldschmidt-Clermont, P. J., Furman, M. I., Wachsstock, D., Safer, D., Nachmias, V. T., and Pollard, T. D. (1992) *Mol. Biol. Cell* **3,** 1015–1024
34. Lindberg, U., Schutt, C. E., Hellsten, E., Tjader, A.-C., and Hult, T. (1988) *Biochim. Biophys. Acta* **967,** 391–400
35. Bershadsky, A. D., Gluck U., Densidenko, O. N., Sklyarova, T. V., Spector, I., and Ben-Ze'ev, A. (1995) *J. Cell Sci.* **108,** 1183–1193
36. De La Cruz, E. M., and Pollard, T. D. (1996) *Biochemistry* **35,** 14054–14061
37. Pantaloni, D., Hill, T. L., Carlier, M.-F., and Korn, E. D. (1985) *Proc. Natl. Acad. Sci. U. S. A.* **82,** 7207–7211
38. Oosawa, F., and Kasai, M. (1962) *J. Mol. Biol.* **4,** 10–21